# Initial Events during the Evolution of $C_4$ Photosynthesis in $C_3$ Species of *Flaveria*[1][W][OPEN]

**Tammy L. Sage*, Florian A. Busch[2], Daniel C. Johnson, Patrick C. Friesen, Corey R. Stinson, Matt Stata, Stefanie Sultmanis, Beshar A. Rahman, Stephen Rawsthorne, and Rowan F. Sage**

Department of Ecology and Evolutionary Biology, University of Toronto, Toronto, Ontario M5S3B2, Canada (T.L.S., F.A.B., D.C.J., P.C.F., C.R.S., M.S., S.S., B.A.R., R.F.S.); and John Innes Centre, Norwich Research Park, Colney, Norwich NR4 7UH, United Kingdom (S.R.)



The evolution of $C_4$ photosynthesis in many taxa involves the establishment of a two-celled photorespiratory $CO_2$ pump, termed $C_2$ photosynthesis. How $C_3$ species evolved $C_2$ metabolism is critical to understanding the initial phases of $C_4$ plant evolution. To evaluate early events in $C_4$ evolution, we compared leaf anatomy, ultrastructure, and gas-exchange responses of closely related $C_3$ and $C_2$ species of *Flaveria*, a model genus for $C_4$ evolution. We hypothesized that *Flaveria pringlei* and *Flaveria robusta*, two $C_3$ species that are most closely related to the $C_2$ *Flaveria* species, would show rudimentary characteristics of $C_2$ physiology. Compared with less-related $C_3$ species, bundle sheath (BS) cells of *F. pringlei* and *F. robusta* had more mitochondria and chloroplasts, larger mitochondria, and proportionally more of these organelles located along the inner cell periphery. These patterns were similar, although generally less in magnitude, than those observed in the $C_2$ species *Flaveria angustifolia* and *Flaveria sonorensis.* In *F. pringlei* and *F. robusta*, the $CO_2$ compensation point of photosynthesis was slightly lower than in the less-related $C_3$ species, indicating an increase in photosynthetic efficiency. This could occur because of enhanced refixation of photorespired $CO_2$ by the centripetally positioned organelles in the BS cells. If the phylogenetic positions of *F. pringlei* and *F. robusta* reflect ancestral states, these results support a hypothesis that increased numbers of centripetally located organelles initiated a metabolic scavenging of photorespired $CO_2$ within the BS. This could have facilitated the formation of a glycine shuttle between mesophyll and BS cells that characterizes $C_2$ photosynthesis.

$C_4$ photosynthesis reduces the deleterious effects of photorespiration by localizing Rubisco to an internal compartment into which $CO_2$ is concentrated. It has independently evolved more than 62 times in the plant kingdom, making it one of the most convergent of complex traits in the biosphere (Sage et al., 2011a). Studies of $C_4$ evolution have led to conceptual models proposing a stepwise origin of the $C_4$ pathway (Monson and Rawsthorne, 2000; Sage et al., 2012). These models are based on physiological and phylogenetic research with genera that include $C_3$, $C_4$, and $C_3$-$C_4$ intermediate species (Brown et al., 1983; Hattersley et al., 1986; Ku et al., 1991; McKown et al., 2005; Marshall et al., 2007; Muhaidat et al., 2011; Sage et al., 2011b; Christin et al., 2012). Comparisons between groups indicate that photorespiratory $CO_2$ recycling, termed $C_2$ photosynthesis, is an important intermediate phase in the evolution of $C_4$ photosynthesis in many of the $C_4$ lineages (Monson and Rawsthorne, 2000; Sage et al., 2012). In $C_2$ photosynthesis, the photorespiratory enzyme glycine decarboxylase (GDC) is localized to an interior compartment, generally the inner half of bundle sheath (BS) cells. GDC is a mitochondria-specific enzyme, and its location within the BS of $C_2$ species is due to the positioning of most mitochondria along the centripetal wall of the BS cells. This shift in GDC expression forces Gly formed during photorespiration in the mesophyll (M) to migrate into the inner BS for metabolic processing by GDC (Monson et al., 1984; Monson and Rawsthorne, 2000). Under conditions promoting photorespiration, as would occur in hot environments, substantial amounts of $CO_2$ are released in the BS, raising its $CO_2$ concentration two to four times above the atmospheric value (Bauwe et al., 1987; von Caemmerer, 1989). Chloroplast numbers are enhanced in the BS of $C_2$ species, and many of these occur along the inner wall in close association with the BS mitochondria (Brown and Hattersley, 1989; Rawsthorne, 1992; Marshall et al., 2007; Muhaidat et al., 2011; Sage et al., 2011b). This organelle arrangement allows for rapid reassimilation of $CO_2$ released by BS GDC (Monson and Rawsthorne, 2000). As a consequence, Rubisco efficiency and photosynthetic capacity are enhanced in environments promoting photorespiration (Schuster and Monson, 1990; Monson and Jaeger, 1991; Dai et al., 1996; Vogan et al., 2007).

[1] This work was supported by the Natural Science and Engineering Research Council of Canada (grant nos. 155258–2008 to T.L.S. and 154273–2012 to R.F.S.) and by the Biotechnology and Biological Sciences Research Council (to S.R.).

[2] Present address: Research School of Biology, Australian National University, Canberra, Australian Capital Territory 0200, Australia.

* Address correspondence to tammy.sage@utoronto.ca.

The author responsible for distribution of materials integral to the findings presented in this article in accordance with the policy described in the Instructions for Authors (www.plantphysiol.org) is: Tammy L. Sage (tammy.sage@utoronto.ca).

[W] The online version of this article contains Web-only data.

[OPEN] Articles can be viewed online without a subscription.

www.plantphysiol.org/cgi/doi/10.1104/pp.113.221119

 

The evolution of the $C_2$ pathway has been proposed to be essential for the subsequent rise of $C_4$ photosynthesis, because many components of the $C_4$ pathway are present in $C_2$ plants that are closely related to $C_4$ species (Rawsthorne, 1992; Monson and Rawsthorne, 2000; Sage et al., 2012). For example, enlarged, Kranz-like BS cells with increased organelle number, rapid M-to-BS trafficking networks, and increased vein density are present in $C_2$ species (Brown et al., 1983; Brown and Hattersley, 1989; Marshall et al., 2007; McKown and Dengler, 2007; Muhaidat et al., 2011; Sage et al., 2011b). An improved understanding of why, and how, the $C_2$ pathway evolved could thus be important for understanding how $C_4$ plants originated and why they did so with such high frequency. A means to study $C_2$ evolution is to examine $C_3$ species that are closely related to $C_2$ species within a phylogenetic clade, for example, in *Flaveria* and *Sartwellia*, two sister genera in the subtribe Flaveriinae of the Asteraceae (McKown et al., 2005). The genus *Flaveria* has long served as the biochemical and physiological model for $C_4$ evolution, and its phylogenetic relationships have been resolved in recent years (Powell, 1978; Monson and Rawsthorne, 2000; McKown et al., 2005; Kapralov et al., 2011). The genus is known to contain nine $C_2$ species, eight $C_4$ species, and three accepted $C_3$ species (McKown et al., 2005); a fourth $C_3$ species, *Flaveria mcdougallii*, is of uncertain taxonomic affinity and is not available due to its rarity. The $C_3$ species *Flaveria cronquistii*, *Flaveria pringlei*, and *Flaveria robusta* are sister to the $C_2$ *Flaveria* species (Fig. 1). *F. cronquistii* branches at a basal node within the *Flaveria* phylogeny, while *F. pringlei* branches at a node between *F. cronquistii* and *F. robusta*. *F. robusta* branches between *F. pringlei* and the node where the $C_2$ and $C_4$ clades of the genus *Flaveria* arise (McKown et al., 2005). *F. pringlei* and *F. robusta* may thus be good representatives of the last common ancestor between the $C_3$ and $C_2$ species within the genus *Flaveria*. Along with *Sartwellia*, the sister genus to *Flaveria*, these $C_3$ species represent an ideal opportunity to study trait changes within a $C_3$ clade where $C_4$ evolution was initiated.

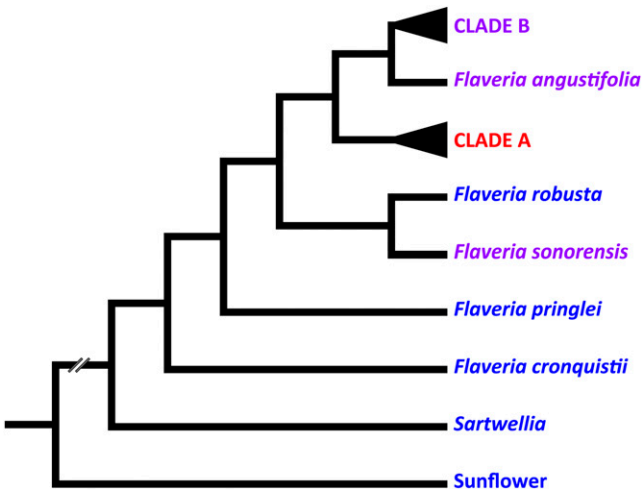


**Figure 1.** A simplified version of the composite Flaveriinae phylogeny of McKown et al. (2005) showing the relative branch points of the species used in this study. Species previously characterized as $C_3$ species are indicated in blue; $C_2$ species and the predominantly $C_2$ clade B are shown in purple; the predominantly $C_4$ clade A is shown in red.

The conclusion that *F. cronquistii*, *F. pringlei*, and *F. robusta* are functionally $C_3$ species is based on many gas-exchange, biochemical, and anatomical studies (Holaday et al., 1984; Brown and Hattersley, 1989; Ku et al., 1991; Dai et al., 1996; McKown and Dengler, 2007). No study has rigorously described the ultrastructure and GDC and Rubisco enzyme localization of these species, however. Such an examination is warranted given that important early events postulated for $C_4$ evolution may occur in BS cells during the transition from full $C_3$ to $C_2$-like photosynthesis (Sage et al., 2012). For example, in *Steinchisma laxa*, a $C_3$ relative of the $C_2$ species of *Steinchisma* (Poaceae), and in $C_3$ relatives of $C_2$ species in *Heliotropium* (Boraginaceae), BS mitochondria have shifted to the inner, centripetal pole of the BS cells (Brown et al., 1983; Muhaidat et al., 2011). $C_3$ *Salsola* species (Chenopodiaceae) that are closely related to $C_4$ clades also exhibit mitochondrial shifts to the inner BS (Voznesenskaya et al., 2013). These observations indicate that there is a distinct early phase of $C_4$ evolution termed "proto-Kranz," where enlarged BS cells have increased numbers of mitochondria in a centripetal position (Muhaidat et al., 2011; Sage et al., 2012). If this is correct, then it is possible that *F. pringlei* and/or *F. robusta*, the two $C_3$ species of *Flaveria* that are most closely related to the $C_2$ species, also exhibit proto-Kranz traits. One of the $C_3$ *Flaveria* species (*F. pringlei*) has been noted to have high organelle numbers in the BS, although no data were presented (Holaday and Chollet, 1984). McKown and Dengler (2007), by contrast, note the BS cells of $C_3$ *Flaveria* species are largely free of chloroplasts.

To evaluate the early events in the evolution of $C_4$ photosynthesis, this research examines the cell biology and leaf gas exchange of three $C_3$ *Flaveria* species, two $C_2$ *Flaveria* species that are immediate sisters of the $C_3$ species, and *Sartwellia flaveriae*, from the sister genus to *Flaveria* in the Flaveriinae. We also examined the $C_3$ plant sunflower (*Helianthus annuus*), a fellow member of the tribe Helianatheae. We specifically evaluated the hypothesis that *F. pringlei* and *F. robusta* exhibit proto-Kranz characteristics that could be considered to be rudimentary features of $C_2$ metabolism, as found in the $C_2$ species in the study, *Flaveria angustifolia* and *Flaveria sonorensis*. If the hypothesis is supported, the results would enhance our understanding of the earliest developments in the evolution of $C_4$ photosynthesis and could clarify why this complex trait has evolved so frequently in the plant kingdom.

## RESULTS

To statistically evaluate whether *F. pringlei* and *F. robusta* exhibit intermediate characteristics between typical

$C_3$ and $C_2$ plants, we placed the seven species of this study into three functional groups. Sunflower, *S. flaveriae*, and *F. cronquistii* represent the first group of typical or pure $C_3$ species. *F. pringlei* and *F. robusta* represent a second group we term proto-Kranz. *F. angustifolia* and *F. sonorensis* make up the third group of $C_2$ species. Data means for these functional categories are presented in Tables I and II along with the species means.

### BS Anatomy and Ultrastructure

The classical view of BS cells in $C_3$ plants is that they are small with few organelles (Metcalfe and Chalk, 1979; Sage, 2004). As a representative of a typical $C_3$ phenotype, we selected sunflower, which is in the same taxonomic tribe as *Flaveria* spp. and *S. flaveriae*. In sunflower, minor veins and adjacent BS cells lack prominence within the M tissue, due in part to the small size of the BS cells (Fig. 2). Sunflower BS cells are one-fourth to one-third the size of BS cells in *S. flaveriae* and *F. cronquistii*, yet they have similar organelle numbers and coverage as these Flaveriinae species (Tables I and II). The sunflower chloroplasts are preferentially in the outer half of the BS cell, where they are positioned along the intercellular air space (IAS; Fig. 2; Table II). In sunflower, similar proportions of the BS cell perimeters face M cells, IAS, other BS cells, and vascular tissue (Table I).

In *S. flaveriae* and *F. cronquistii*, BS cells are on average enlarged relative to sunflower and the other *Flaveria* species, and many of their larger BS cells extend into the IAS (Fig. 3, A and B; Table I; Supplemental Fig. S1). In *S. flaveriae*, more than one-third of the BS cell perimeter faces the IAS (Table I). In *F. cronquistii*, 16% of the BS perimeter faces the IAS. By contrast, in *F. pringlei*, *F. robusta*, *F. sonorensis*, and *F. angustifolia*, the BS cells have less IAS exposure, averaging less than 15%, while exposure of a BS cell to adjacent BS cells is high, exceeding 35% (Table I). These results indicate the BS tissue of these four *Flaveria* species form more of a radial sheath than is observed in *S. flaveriae* and *F. cronquistii*.

In the BS, chloroplast and mitochondria numbers increase in the species of this study that branch at more distal nodes in the *Flaveria* phylogeny (Table II; Fig. 1). The relative number of BS chloroplasts in the $C_2$ species is more than twice that in sunflower, *S. flaveriae*, and *F. cronquistii*. Chloroplast numbers in the BS of *F. pringlei* and *F. robusta* were 50% higher than in these typical $C_3$ species. In both the proto-Kranz and $C_2$ species, there are almost twice as many BS mitochondria than in the typical $C_3$ species (Table II). Chloroplast size differs little between the species, while mitochondria are larger in the proto-Kranz and $C_2$ species. These changes in number and/or size of the chloroplasts and mitochondria lead to greater coverage of the BS cell area by these organelles in cross section in the $C_2$ species and, in the case of mitochondrial coverage, for the proto-Kranz species as well. Unlike sunflower, the BS chloroplasts in *F. pringlei*, *F. robusta*, *F. sonorensis*, and *F. angustifolia* are evenly distributed between inner and outer halves of the BS cells (Table II). In *Flaveria* spp., there is an increase in the mitochondria numbers in the inner half of the BS cell relative to the more uniform distribution in sunflower and *S. flaveriae*. Close to 90% of the mitochondria are on the inner half of the BS cells in *F. pringlei*, *F. robusta*, *F. sonorensis*, and *F. angustifolia*, where they form a distinct row along the inner cell periphery (Table II; Figs. 3 and 4). Chloroplast coverage in the inner half of the BS exceeds 12% in the two $C_2$ species and averages 5.9% in *F. pringlei* and *F. robusta* (Table II). Such an aggregation is absent in the typical $C_3$ species, where chloroplast coverage averages 2.4% of the inner BS (Table II). In the proto-Kranz and $C_2$ species, the inner chloroplasts are positioned against the rank of mitochondria lining the inner BS wall (Figs. 3, C–F, and 4, C–F), in a pattern that is typical for $C_2$ species (Monson and Rawsthorne, 2000). In the proto-Kranz and $C_2$ species, the outer chloroplasts have no consistent association with mitochondria. By contrast, BS mitochondria in sunflower, *S. flaveriae*, and *F. cronquistii* are close to chloroplasts when positioned along the cell periphery

**Table I.** *The cross-section area and perimeter of BS cells, and the percentage of BS cell perimeter in contact with other BS cells, M cells, or the IAS of five Flaveria species, S. flaveriae, and sunflower*

Means ± SE are given; $n = 3$ to 4 plants per species. Letters indicate statistically distinct means between species or photosynthetic groups using one-way ANOVA and the Student-Newman-Keuls post-hoc test. Species means were tested separately from photosynthetic type means. PK, Proto-Kranz.

| Species | Area per BS Cell | BS Cell Perimeter | Percentage of BS Cell Perimeter Facing BS | Percentage of BS Cell Perimeter Facing M | Percentage of BS Cell Perimeter Facing IAS |
|---|---|---|---|---|---|
| | $\mu m^2$ | $\mu m$ | | | |
| Sunflower ($C_3$) | 578 ± 58 a | 95 ± 5 a | 23.6 ± 0.6 a | 25.4 ± 2.5 a | 25.5 ± 0.4 b |
| *S. flaveriae* ($C_3$) | 2,221 ± 343 b | 182 ± 16 b | 22.8 ± 2.2 a | 22.4 ± 2.9 a | 37.4 ± 6.6 c |
| *F. cronquistii* ($C_3$) | 1,639 ± 405 a,b | 150 ± 20 a,b | 30.0 ± 2.8 a,b | 38.2 ± 1.9 b | 16.3 ± 4.2 a,b |
| $C_3$ average | 1,480 ± 286 x | 142 ± 15 x | 25.5 ± 1.5 x | 28.7 ± 2.7 x | 26.4 ± 3.8 y |
| *F. pringlei* (PK) | 1,044 ± 230 a | 121 ± 16 a | 35.4 ± 3.5 b | 37.5 ± 2.0 b | 9.9 ± 3.0 a |
| *F. robusta* (PK) | 748 ± 100 a | 105 ± 8 a | 37.1 ± 2.8 b,c | 33.3 ± 2.7 a,b | 4.5 ± 1.6 a |
| Proto-Kranz average | 917 ± 142 x | 114 ± 9 x | 36.1 ± 2.2 y | 35.7 ± 1.7 x | 7.6 ± 2.0 x |
| *F. angustifolia* ($C_2$) | 913 ± 170 a | 116 ± 7 a | 45.8 ± 2.9 c | 28.2 ± 3.6 a,b | 6.4 ± 2.1 a |
| *F. sonorensis* ($C_2$) | 1,034 ± 53 a | 124 ± 3 a | 39.8 ± 1.6 b,c | 27.4 ± 1.4 a | 14.5 ± 2.5 a,b |
| $C_2$ average | 983 ± 74 x | 121 ± 4 x | 42.4 ± 1.8 z | 27.7 ± 1.6 x | 11.1 ± 2.3 x |

**Table II.** *Characteristics of bundles sheath organelles from sunflower, S. flaveriae, and species of Flaveria*

Means ± SE are given; $n = 3$ to 4 plants per species. Letters indicate statistically distinct means via one-way ANOVA and the Student-Newman-Keuls post-hoc test ($P < 0.05$). Species means were tested separately from photosynthetic type means. PK, Proto-Kranz.

| Species | Relative No. (per $\mu m^{-2} \times 10^{-3}$) | Size | Proportion in Inner Half of Cell | Coverage of Total Cell Area | Coverage of Inner Half of Cell Area |
|---|---|---|---|---|---|
| | | $\mu m^2$ | % | % | % |
| BS chloroplast | | | | | |
| Sunflower ($C_3$) | 8.0 ± 1.4 a | 4.8 ± 0.5 a | 21.8 ± 3.6 a | 3.9 ± 1.0 a | 1.6 ± 0.2 a |
| *S. flaveriae* ($C_3$) | 8.6 ± 1.0 a | 4.4 ± 0.3 a | 47.1 ± 7.3 b,c | 3.8 ± 0.6 a | 2.5 ± 0.5 a |
| *F. cronquistii* ($C_3$) | 7.9 ± 1.1 a | 4.1 ± 0.6 a | 37.8 ± 5.9 b | 3.0 ± 0.2 a | 3.1 ± 0.6 a |
| $C_3$ average | 8.2 ± 0.6 x | 4.4 ± 0.3 x | 35.6 ± 4.7 x | 3.6 ± 0.4 x | 2.4 ± 0.3 x |
| *F. pringlei* ($C_3$ PK) | 12.6 ± 1.9 a | 4.0 ± 0.3 a | 49.2 ± 2.7 b,c | 4.8 ± 0.5 a | 4.4 ± 0.6 a |
| *F. robusta* ($C_3$ PK) | 13.5 ± 2.3 a | 4.7 ± 1.4 a | 56.4 ± 2.9 c | 6.9 ± 3.3 a,b | 7.9 ± 4.3 a,b |
| Proto-Kranz average | 13.0 ± 1.4 y | 4.3 ± 0.6 x | 52.3 ± 2.3 y | 5.7 ± 1.3 x | 5.9 ± 1.8 y |
| *F. angustifolia* ($C_2$) | 20.1 ± 1.5 b | 5.1 ± 0.1 a | 59.7 ± 3.7 c | 10.2 ± 0.8 b | 12.1 ± 1.2 b |
| *F. sonorensis* ($C_2$) | 21.0 ± 1.1 b | 5.6 ± 0.2 a | 60.4 ± 2.6 d | 11.5 ± 1.0 b | 15.2 ± 1.6 b |
| $C_2$ average | 20.6 ± 0.8 z | 5.4 ± 0.2 x | 60.1 ± 2.0 y | 10.9 ± 0.7 y | 13.9 ± 1.2 z |
| BS mitochondria | | | | | |
| Sunflower ($C_3$) | 15.4 ± 3.6 a,b | 0.3 ± 0.02 a | 56.7 ± 1.9 a | 0.4 ± 0.1 a | 0.4 ± 0.1 a |
| *S. flaveriae* ($C_3$) | 7.9 ± 0.9 a | 0.4 ± 0.04 a | 52.9 ± 10.4 a | 0.3 ± 0.1 a | 0.6 ± 0.1 a |
| *F. cronquistii* ($C_3$) | 9.1 ± 2.7 a | 0.4 ± 0.02 a | 72.5 ± 2.9 b | 0.4 ± 0.1 a | 0.5 ± 0.2 a |
| $C_3$ average | 10.8 ± 1.8 x | 0.4 ± 0.03 x | 60.8 ± 4.4 x | 0.4 ± 0.1 x | 0.5 ± 0.1 x |
| *F. pringlei* ($C_3$ PK) | 18.0 ± 3.3 a,b | 0.5 ± 0.01 a | 86.0 ± 2.1 b | 0.9 ± 0.1 a,b | 1.4 ± 0.3 a,b |
| *F. robusta* ($C_3$ PK) | 18.4 ± 3.2 a,b | 0.7 ± 0.2 a,b | 90.1 ± 3.1 b | 1.2 ± 0.1 b | 2.1 ± 0.1 b |
| Proto-Kranz average | 18.2 ± 2.1 y | 0.6 ± 0.1 y | 87.8 ± 1.8 y | 1.0 ± 0.1 y | 1.7 ± 0.2 y |
| *F. angustifolia* ($C_2$) | 16.3 ± 2.3 a,b | 0.7 ± 0.1 a,b | 86.3 ± 2.2 b | 1.2 ± 0.3 b | 2.1 ± 0.6 b |
| *F. sonorensis* ($C_2$) | 22.4 ± 2.1 b | 1.0 ± 0.1 b | 89.8 ± 1.8 b | 2.1 ± 0.2 c | 4.1 ± 0.4 c |
| $C_2$ average | 19.8 ± 1.9 y | 0.9 ± 0.1 z | 88.3 ± 1.5 y | 1.7 ± 0.2 z | 3.2 ± 0.5 z |

facing the IAS, yet they are scattered and often have no chloroplast nearby when positioned along the cell periphery facing another cell (Figs. 2 and 3, A and B).

### M Properties

In all species studied, the M organelles occur on the cell periphery, usually opposite the intercellular air spaces. Mitochondria were generally associated with M chloroplasts. Organelles were equally distributed around the M cell periphery facing the IAS, demonstrating no polar separation as occurs in the BS cells of $C_2$ species (Supplemental Table S1). Chloroplast and mitochondrial numbers per M cell area were similar in all species. With the exception of sunflower, which had larger chloroplasts and chloroplast coverage of the M cell area, there was no significant variation between the species in chloroplast or mitochondrial coverage of the M cell area (Supplemental Table S1). These results demonstrate that observed changes in BS organelle numbers and distribution are unique to BS cells rather than reflecting altered patterning in all photosynthetic cells.

### Immunolocalization of Rubisco and GDC

Immunolocalizations show the presence of the P-subunit of GDC (GDCp) and the Rubisco large subunit as brown stain corresponding to the location of either mitochondria (for GDCp) or chloroplasts (for Rubisco). The label indicating Rubisco appears throughout the leaves of the five *Flaveria* species; however, there are distinct bands of Rubisco label around the inner BS regions in *F. pringlei* and *F. robusta* and the $C_2$ species *F. angustifolia* and *F. sonorensis* (Supplemental Fig. S2). Such banding is not pronounced in the inner BS of *F. cronquistii*. Immunolabel indicates that GDCp is present throughout the M tissue of *F. cronquistii*, although the label intensity is reduced in the M cells in the middle of the leaf (Fig. 5). The label for GDCp is present as distinct, punctate dots along the M cell periphery, which is consistent with the location of mitochondria in the M tissues (Muhaidat et al., 2011). BS cells lack pronounced GDCp stain in *F. cronquistii*. In *F. pringlei* and *F. robusta*, GDCp label is apparent throughout the M tissue, while in the BS, a distinct though narrow band of GDCp stain is apparent along the centripetal walls of the cells (Fig. 6, A and B); at high magnification, this GDCp label is evident as a row of punctate spots corresponding to the position of the mitochondria (Supplemental Fig. S3). The BS cells of *F. sonorensis* and *F. angustifolia* have a very pronounced band of GDCp immunolabel in the inner BS region, where the large majority of the BS mitochondria occur (Fig. 6, C and D; Supplemental Fig. S3). Both *F. sonorensis* and *F. angustifolia* exhibit punctate spots of GDCp label in the M tissue, although it is noticeably less than in the $C_3$ *Flaveria* species, particularly in the lower and interior regions of the M tissue (Fig. 6, C and D; Supplemental Fig. S4). By comparison, the $C_2$ species *Flaveria floridana* shows little GDCp immunolabel in the M tissue, in contrast to pronounced label being present in the inner BS cells (Supplemental Fig. S4E).

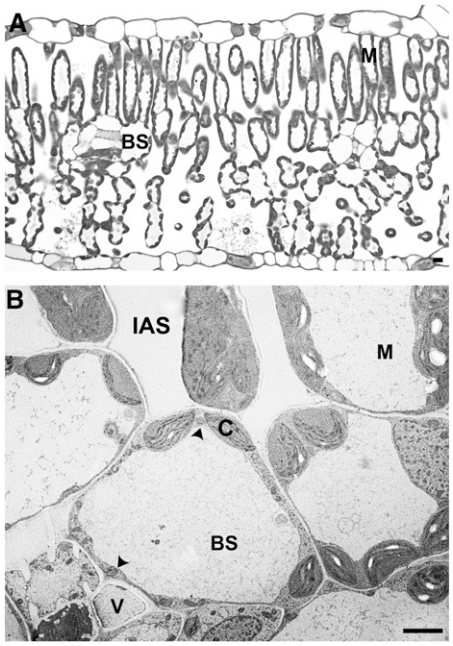


**Figure 2.** Light (A) and transmission (B) electron micrographs of leaf cross sections of sunflower illustrating BS cells and their organelles. Arrowheads indicate mitochondria. C, Chloroplast; M, mesophyll; V, vascular tissue. Bars = 5 $\mu$m.

### Leaf Gas Exchange

The $CO_2$ compensation point of the net $CO_2$ assimilation rate ($\Gamma$) declined as light intensity increased above darkness in the $C_2$, proto-Kranz, and $C_3$ species (Fig. 7). Each group exhibited similar $\Gamma$ values at a photon flux density below 150 $\mu$mol $m^{-2}$ $s^{-1}$, while above 150 $\mu$mol $m^{-2}$ $s^{-1}$, the $\Gamma$ values in the $C_2$ species are 35 to 39 $\mu$mol $mol^{-1}$ lower than in the $C_3$ species. At saturating light (1,000–1,400 $\mu$mol $m^{-2}$ $s^{-1}$), $\Gamma$ is on average 4 to 10 $\mu$mol $mol^{-1}$ lower in the proto-Kranz *F. pringlei* and *F. robusta* than in *F. cronquistii* and *S. flaveriae* (Fig. 7).

In the three typical $C_3$ species (sunflower, *S. flaveriae*, and *F. cronquistii*) and in *F. pringlei*, the response slopes of the net $CO_2$ assimilation rate ($A$) versus intercellular $CO_2$ content ($C_i$) curves determined at multiple light intensities converge upon a common value, which was used to estimate the apparent $CO_2$ compensation point ($C^*$) in the absence of apparent mitochondrial respiration in the light ($R_d$; Fig. 8, A–C; data not shown for sunflower). The apparent $R_d$ values corresponding to the species $C^*$ estimates are indicated by dashed lines in Figure 8. In *F. robusta* and the $C_2$ species *F. sonorensis* and *F. angustifolia*, the $A/C_i$ responses measured at the low to intermediate light intensities roughly converge on a common intercept, allowing for an approximate $C^*$ estimate. The $A/C_i$ responses at saturating light are shifted to higher $A$ values at each $C_i$ value, such that they do not converge on the estimated $C^*$ but instead intercept the $R_d$ line at a lower value than $C^*$ (Fig. 8, D–F, compare gray and black arrows). At the estimated $R_d$ intercept, the $C_i$ of the high-light curves is statistically the same as $C^*$ in each of the $C_3$ species except *F. robusta*, where it is 2.6 $\mu$mol $mol^{-1}$ less than $C^*$ (Table III). In the $C_2$ species, the high-light $C_i$ at $R_d$ is 14.5 $\mu$mol $mol^{-1}$ less on average than the estimated $C^*$ (Table III). In *F. sonorensis* and *F. angustifolia*, the $R_d$ intercept of the $A/C_i$ response measured at 400 $\mu$mol $m^{-2}$ $s^{-1}$ is also shifted to a lower $C_i$ than the estimated $C^*$, but only by a slight amount (Fig. 8, E and F).

## DISCUSSION

In the BS cells of the species studied here, there is a change in structural traits from a typically $C_3$ pattern

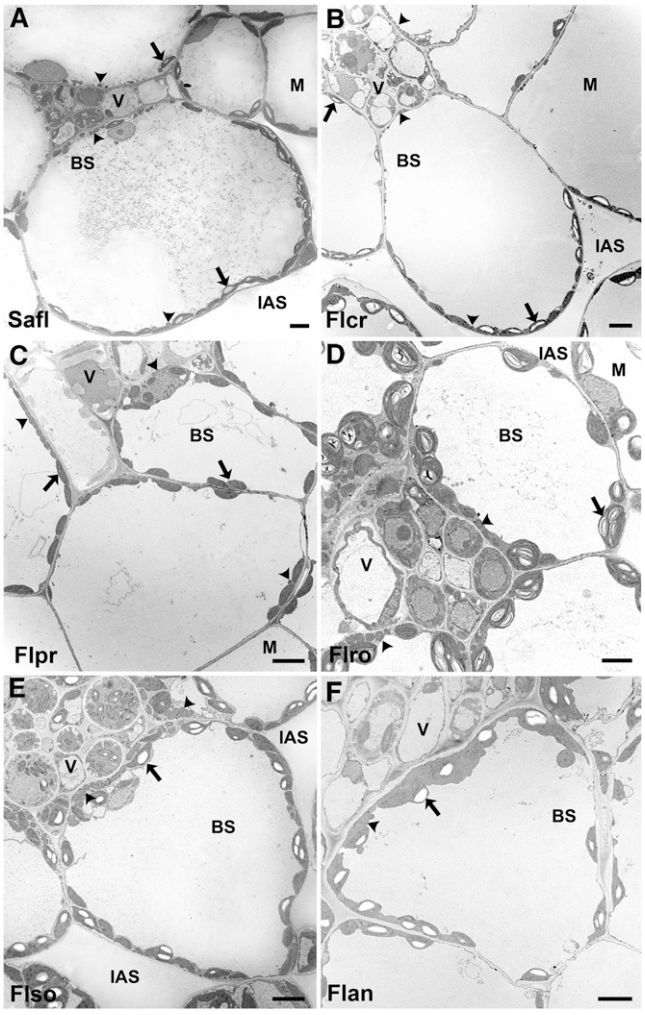


**Figure 3.** Transmission electron micrographs of organelle distribution in BS cells. BS chloroplasts are predominantly situated opposite vascular tissue adjacent to the IAS in *S. flaveriae* (Safl; A) and *F. cronquistii* (Flcr; B) but occupy the outer and inner cell periphery of *F. pringlei* (Flpr; C), *F. robusta* (Flro; D), *F. sonorensis* (Flso; E), and *F. angustifolia* (Flan; F). Arrows mark BS chloroplasts, and arrowheads label BS mitochondria. V, Vascular tissue. For light micrographs of BS and adjacent M tissue, see Supplemental Figure S1 and McKown and Dengler (2007). Bars = 5 $\mu$m.

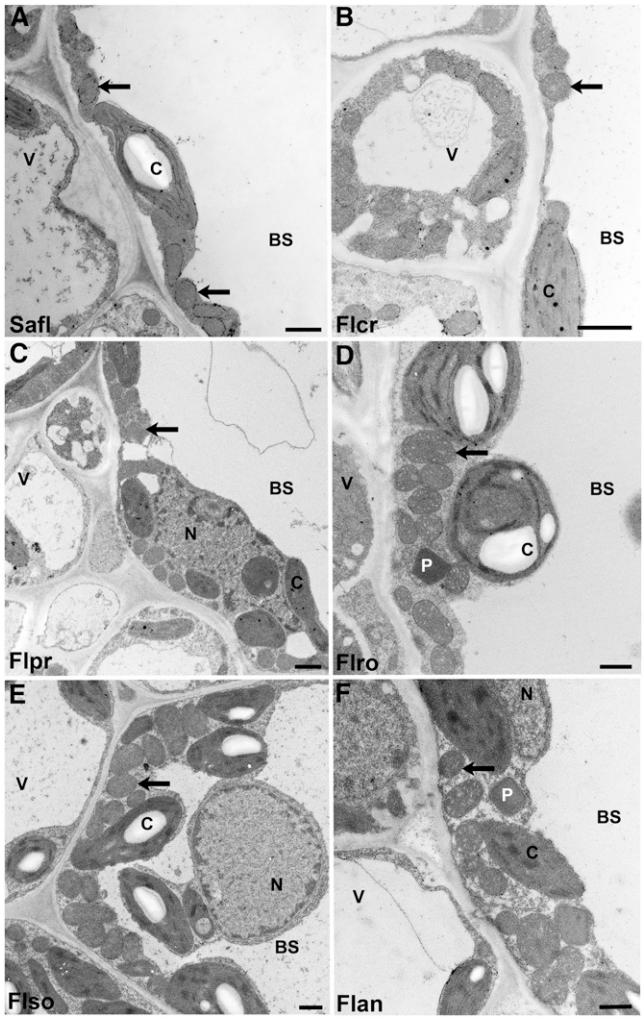


**Figure 4.** Transmission electron micrographs at high magnification of organelle distribution in the inner BS cells in *S. flaveriae* (Safl; A), *F. cronquistii* (Flcr; B), *F. pringlei* (Flpr; C), *F. robusta* (Flro; D), *F. sonorensis* (Flso; E), and *F. angustifolia* (Flan; F). Arrows label mitochondria. C, Chloroplast; N, nucleus; P, peroxisome; V, vascular tissue. Bars = 1 $\mu$m.

in sunflower, *S. flaveriae*, and *F. cronquistii* to an intermediate, $C_2$-like pattern in *F. pringlei* and *F. robusta*. This intermediate cellular state includes an increase in organelle numbers and size as well as a shift in organelle positioning to the centripetal BS pole. These cellular traits, combined with the high vein density and large BS size reported for these species (McKown and Dengler, 2007), demonstrate that *F. pringlei* and *F. robusta* exhibit proto-Kranz features. In combination with the slight reduction in $\Gamma$ and the $C_i$ at which the high-light $A/C_i$ response intercepts the apparent $R_d$ line, these features indicate that the proto-Kranz species are intermediate between the typical $C_3$ and $C_2$ species and likely operate a weak Gly shuttle that enhances photosynthetic efficiency in the BS tissue if not the entire leaf. If the characteristics in these species reflect ancestral states, as suggested by their intermediate branching positions in the genus *Flaveria* phylogeny, the data support the hypothesis that the assembly of the $C_2$ pathway occurs gradually and in its incipient form may be a mechanism to scavenge photorespired $CO_2$. Below, we discuss the series of changes in *Flaveria* spp. that we hypothesize are the initiating steps in $C_2$ evolution and place these results into the context of previous studies and current models of $C_4$ evolution.

### $C_2$ Photosynthesis in *Flaveria* Species

In *F. angustifolia* and *F. sonorensis*, organelle size and number are increased in the BS relative to the typical $C_3$ species, with a large fraction of the organelles occurring at the centripetal pole of the cells. Mitochondria, and thus GDC, are localized along the inner BS wall, where close to 90% of them occur in a line between the plasmalemma and a row of chloroplasts. This pattern is critical because it facilitates the reassimilation of photorespired $CO_2$ via a Gly shuttle from M cells (Hylton et al., 1988; Rawsthorne, 1992). GDC is thought to be absent in the M cells of well-developed $C_2$ species, perhaps as a result of a knockout mutation early in $C_2$ evolution (Rawsthorne, 1992; Sage et al., 2012). Consistently, GDCp is not observed in the M cells of many well-developed $C_2$ species, for example, in the genera *Cleome* (Marshall et al., 2007; Voznesenskaya et al., 2007), *Euphorbia* (Sage et al., 2011b), *Brassica* (Ueno, 2011), and *Heliotropium* (Muhaidat et al., 2011). In *Flaveria* spp., Hylton et al. (1988) observed no significant immunogold labeling for GDCp in M cell mitochondria of the $C_2$ species *Flaveria linearis* and *F. floridana*. We also observed no GDCp label in M mitochondria of *F. floridana* (Supplemental Fig. S4). Recently, it has been suggested that the loss of M GDC during $C_2$ evolution in *Flaveria* spp. is gradual, based on molecular data from $C_2$ *Flaveria chlorifolia* and *Flaveria anomala* that show partial reduction in GDCp transcript abundance in the M tissue relative to $C_3$ *Flaveria* species (Schulze et al., 2013). Our results with *F. angustifolia* and *F. sonorensis* support this possibility, as these two species exhibit immunostaining for GDCp in the M tissue. In the *Flaveria* spp. phylogeny, *F. sonorensis*, *F. angustifolia*, *F. anomala*, and *F. chlorifolia* branch in an intermediate position between the $C_3$ species and *F. linearis* and *F. floridana* (McKown et al., 2005). Thus, in *Flaveria*, GDC loss in the M tissue is incomplete in the basal-branching group of $C_2$ species but becomes complete in the more distal-branching *F. floridana* and *F. linearis*.

Immunolabel for GDCp is associated with GDC activity (Rawsthorne et al., 1988a, 1988b; Rawsthorne, 1992); hence, the GDCp label in the M cells of *F. angustifolia* and *F. sonorensis* indicates that GDC is still active in the M tissue. This could explain, in part, their light dependency of $\Gamma$ for the following reason. At low light, $\Gamma$ values converge in the $C_2$ and $C_3$ species, demonstrating a reduced level of $CO_2$ refixation in the $C_2$ species (Ku et al., 1991; Dai et al., 1996). Ribulose 1,5-bisphosphate regeneration capacity is reduced in low light, which will

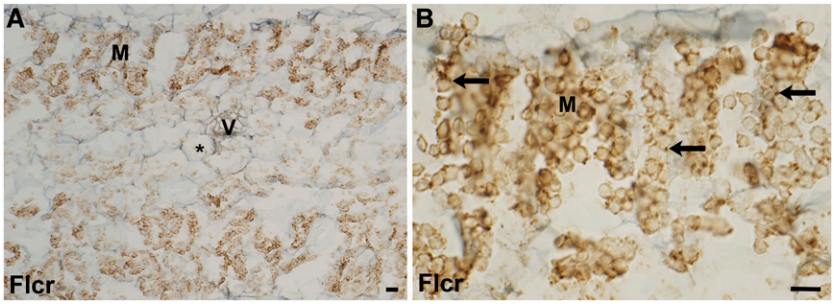


**Figure 5.** In situ immunolocalization of GDCp in the leaf of *F. cronquistii* (Flcr). Arrows mark mitochondria, and the asterisk labels a BS cell. V, Vascular tissue. Bars = 10 $\mu$m.

reduce Rubisco oxygenase activity and, in turn, the rate of Gly formation (von Caemmerer, 1989, 2000). Residual GDC activity in the M cells of these $C_2$ species could metabolize much of the Gly produced at low light, thus reducing the relative flux of Gly into the BS and hence the BS $CO_2$ concentration. As light intensity increases, Gly production increases in the $C_2$ species and presumably exceeds the residual M GDC activity, thereby leading to an overflow of Gly into the BS, causing the BS $CO_2$ concentration to increase and $\Gamma$ to decline.

While $\Gamma$ estimates from $C_2$ species are abundant in the literature (Monson and Rawsthorne, 2000; Vogan et al., 2007; Voznesenskaya et al., 2007), $C^*$ estimates are rare (Voznesenskaya et al., 2010). As an indicator of photorespiratory $CO_2$ refixation, $C^*$ has advantages over the commonly used parameter $\Gamma$. Rubisco carboxylation capacity, $R_d$, $CO_2$ refixation, and the oxygenation-to-carboxylation ratio of Rubisco influence $\Gamma$ (Tholen et al., 2012; Busch et al., 2013), whereas $C^*$ is largely a function of the refixation of (photo)respired $CO_2$ and the oxygenation-to-carboxylation ratio of Rubisco (von Caemmerer, 2000; Busch et al., 2013). All of the *Flaveria* species in this study have similar Rubisco specificity factors and, hence, similar oxygenation potentials (Kubien et al., 2008). Therefore, it can be concluded that the differences in estimated $C^*$ between the $C_3$ and $C_2$ species reflect the greater potential for the refixation of photorespired $CO_2$ in the $C_2$ species (Bauwe et al., 1987; Monson and Rawsthorne, 2000). A previously unrecognized response in $C_2$ species is the reduction in the intercept of the high-light $A/C_i$ response with the $R_d$ line, which is 13 to 14 $\mu$mol mol$^{-1}$ below the $C^*$ estimate in both *F. angustifolia* and *F. sonorensis*. We hypothesize that this reduction in the $R_d$ intercept at high light is caused by an increasing flux of Gly into the BS as ribulose 1,5-bisphosphate regeneration approaches its maximum capacity. Consistent with this hypothesis, we observed a slight downward shift in the $R_d$ intercepts of the $A/C_i$ responses measured at intermediate light intensities in the $C_2$ species.

### *F. pringlei*, *F. robusta*, and the Proto-Kranz Syndrome

Compared with sunflower and *S. flaveriae*, BS mitochondria in *F. pringlei* and *F. robusta* are more numerous and have moved from an even distribution around the cell to a largely centripetal location adjacent to the vascular tissue. This aggregation creates the banding pattern of GDCp stain in the inner BS of *F. pringlei* and *F. robusta*, which is an incipient version of the dense banding produced by the numerous large mitochondria in the inner BS of $C_2$ species (Fig. 6; Marshall et al., 2007; Muhaidat et al., 2011; Sage et al., 2011b). Most of the inner BS chloroplasts in *F. pringlei* and to a greater extent *F. robusta* are adjacent to the row of mitochondria along the inner BS wall, in a pattern that is similar though less extensive than that of *F. sonorensis* and

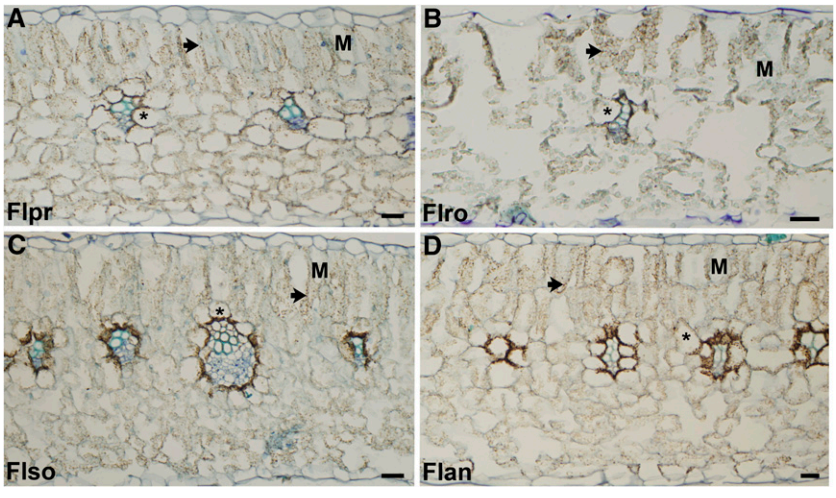


**Figure 6.** In situ immunolocalization of GDCp in leaves of *F. pringlei* (Flpr; A), *F. robusta* (Flro; B), *F. sonorensis* (Flso; C), and *F. angustifolia* (Flan; D). Arrows mark mitochondria, and asterisks label BS cells. For high magnifications of BS and M regions, see Supplemental Figures S3 and S4, respectively. Bars = 20 $\mu$m.

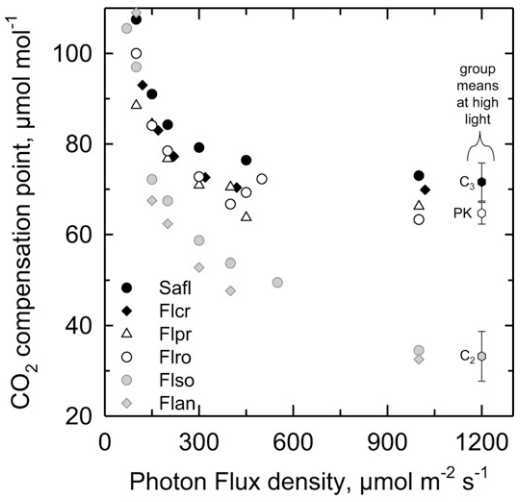


**Figure 7.** The light response of the $CO_2$ compensation point at 36°C in the $C_3$ species *S. flaveriae* (Safl) and *F. cronquistii* (Flcr), the proto-Kranz (PK) species *F. pringlei* (Flpr) and *F. robusta* (Flro), and the $C_2$ species *F. sonorensis* (Flso) and *F. angustifolia* (Flan). Symbols are averages of two to 14 observations, although most samples sizes are four to six. Error bars are shown for group means of all high-light values (1,000 and 1,400 $\mu$mol $m^{-2}$ $s^{-1}$) from the $C_3$, proto-Kranz, and $C_2$ groups. These group means are statistically different at $P < 0.05$ via one-way ANOVA and Holm-Sidak post-hoc test.

*F. angustifolia*. Starch grains and Rubisco are abundant in the inner BS chloroplasts of *F. robusta* and the $C_2$ species, indicating that this region is photosynthetically active. Given the diffusive barrier represented by the vacuole, photosynthetic activity by the inner BS chloroplasts would probably depend upon (photo) respired $CO_2$ released by nearby mitochondria. Similar organellar traits have been observed in the $C_3$ grass *S. laxa* and the $C_3$ borages *Heliotropium karwinskyi* and *Heliotropium procumbens* (Brown et al., 1983; Muhaidat et al., 2011); these species are closely related to $C_2$ species in their respective clades (Aliscioni et al., 2003; Muhaidat et al., 2011). As observed for proto-Kranz *Flaveria* species, *S. laxa*, *H. karwinskyi*, and *H. procumbens* also exhibit increased BS relative to M tissue size and/or increased vein density relative to the typical $C_3$ condition (Morgan and Brown, 1980; Brown et al., 1983; Muhaidat et al., 2011). Notably, enlarged BS cells are a universal condition in the Flaveriinae, as indicated by the relatively large BS cells observed in *S. flaveriae* and *F. cronquistii* (McKown and Dengler, 2007). In the grasses, $C_3$ clades that are sister to $C_4$ clades also have enlarged BS, which together with the observations from *Flaveria* and *Heliotropium* species indicate that this trait may be a common exaptation facilitating the development of $C_2$ and $C_4$ photosynthesis (Sage et al., 2012; Christin et al., 2013; Griffiths et al., 2013). As indicated by *S. laxa*, it is possible that many of the grass species with enlarged BS cells may also have proto-Kranz patterns of organelle numbers and distribution.

The proto-Kranz species measured to date have slightly lower $\Gamma$ than $C_3$ relatives at light saturation, which is consistent with modest refixation of photorespiratory $CO_2$ within the BS (for *S. laxa* $\Gamma$ values, see Supplemental Table S3; Morgan and Brown, 1979; Vogan et al., 2007). *S. laxa* also has a partial loss of M GDCp (compared with a total loss in *Steinchisma hians*; Hylton et al., 1988). The slight reduction of the high-light $A/C_i$ intercept with $R_d$ that we observed in *F. robusta* is further evidence that this species has an enhanced ability to refix photorespired $CO_2$. Our ability to resolve this reduction in the $A/C_i$ by $R_d$ intercept in *F. robusta* but not *F. pringlei* probably reflects a greater refixation capacity in *F. robusta*, due to its higher organelle coverage of the inner BS. Taken together, these observations support the hypothesis that species with proto-Kranz traits operate an incipient form of $C_2$ photosynthesis and are, in essence, $C_3$-$C_2$ intermediates. In its rudimentary form, the $C_2$ cycle may largely be confined to the BS, in what may amount to a single-celled Gly shuttle. The localization of the BS mitochondria to the inner cell would

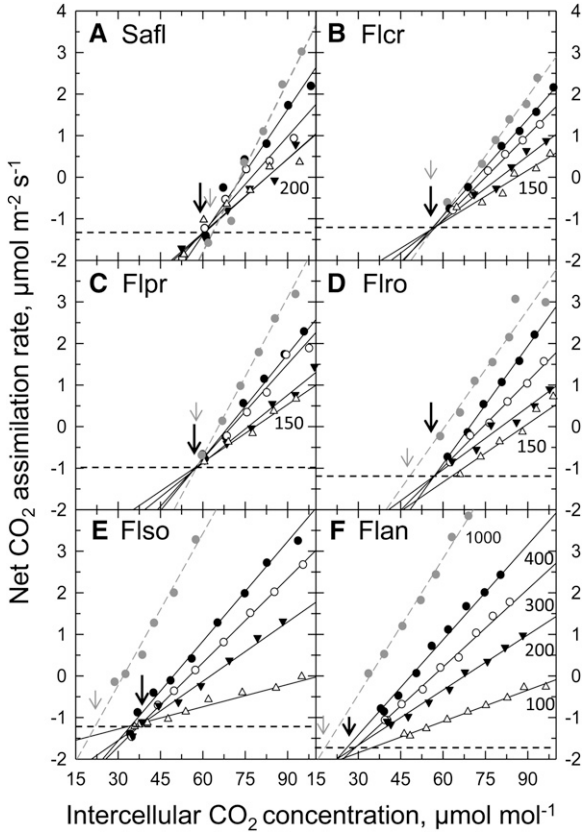


**Figure 8.** Representative responses of *A* to low $C_i$ for *S. flaveriae* (Safl; A), *F. cronquistii* (Flcr; B), *F. pringlei* (Flpr; C), *F. robusta* (Flro; D), *F. sonorensis* (Flso; E), and *F. angustifolia* (Flan; F) at different light intensities. All responses in each panel were generated from a single leaf in a single measurement sequence, beginning with the high-light responses and ending with the lowest. Measurement light intensities are given in F or, if different, beside the respective responses.

**Table III.** *The $C_i$ in leaves of sunflower and species of the Flaveriinae corresponding to the point where (1) the high-light A versus $C_i$ curve intersects the estimated $R_d$ value, (2) multiple low-light A versus $C_i$ curves converge at $R_d$ (=C*), and (3) the difference between the values of 2 and 1 ($\Delta$ =C* − high-light $C_i$ at $R_d$)*

Means ± SE are given, with letters indicating statistically different groups at $P < 0.05$ by one-way ANOVA and the Student-Newman-Keuls post-hoc test. Measurements were determined at 36°C. For examples of how these values where determined, see Figure 7. Values from the $C_3$ species sunflower, *S. flaveriae*, and *F. cronquistii* are pooled together to give a mean of fully expressed or "typical" $C_3$ photosynthesis. The $C_2$ values are pooled from measurements of *F. sonorensis* and *F. angustifolia*. For averages of each of the species, see Supplemental Table S2. PK, Proto-Kranz.

| Species | No. | High-Light $C_i$ at $R_d$ | C* | Difference |
|---|---|---|---|---|
| | | | $\mu$mol mol$^{-1}$ | |
| Pooled $C_3$ average | 2 | 60.6 ± 0.6 c | 60.0 ± 0.6 b | −0.6 ± 0.5 a |
| *F. pringlei* (PK) | 5 | 56.9 ± 0.9 b,c | 57.1 ± 1.3 b | 0.4 ± 0.5 a,b |
| *F. robusta* (PK) | 15 | 55.0 ± 1.1 b | 57.6 ± 1.0 b | 2.6 ± 0.6 b |
| Pooled $C_2$ average | 14 | 22.5 ± 1.5 a | 37.0 ± 1.4 a | 14.5 ± 0.9 c |

force Gly formed in the outer BS to diffuse into the inner BS for metabolism by GDC. The large vacuole would then slow the efflux of the photorespired $CO_2$, enhancing the efficiency of Rubisco in nearby chloroplasts. If the inner BS represents a large enough sink for Gly, this arrangement could also metabolize any Gly that may overflow from the M cells, such as during hot periods when photorespiration may be particularly high.

The Flaveriinae species in this study occur in semiarid landscapes of central Mexico and Texas, where summer temperatures regularly exceed 35°C, humidity is low, and drought is common (Powell, 1978; Sudderth et al., 2009). In recent geological time, heat and aridity would have combined with low atmospheric $CO_2$ to depress $C_i$ and greatly increase photorespiratory potentials in the $C_3$ Flaveriinae species. In the late Pleistocene, for example, the combination of atmospheric $CO_2$ levels near 200 $\mu$mol mol$^{-1}$ and low stomatal conductance could have resulted in $C_i$ values of 120 to 140 $\mu$mol mol$^{-1}$ in hot, low-humidity environments (Sage et al., 2012). Based on our $A/C_i$ responses, a $\Gamma$ reduction of 4 to 10 $\mu$mol mol$^{-1}$ would be sufficient to raise $A$ at a $C_i$ of 120 to 140 $\mu$mol mol$^{-1}$ by 15% to 20%. An improvement of $A$ by this degree under carbon-deficient conditions should have significant consequences in terms of improved fitness and competitive ability (Gerhart and Ward, 2010).

### What Facilitates the Origin of the Proto-Kranz Condition? A Working Hypothesis

As shown by sunflower, the typical BS cells in $C_3$ plants are relatively small, with a few centrifugal chloroplasts and little potential for refixation of photorespired $CO_2$. In *S. flaveriae* and *F. cronquistii*, BS cells have become enlarged relative to sunflower and have many starch-containing chloroplasts facing the IAS, indicating that they assimilate $CO_2$ directly from the IAS, as is typical for M chloroplasts of $C_3$ plants. We conclude from this that the enlarged BS cells of these species have increased their photosynthetic engagement. Similar patterns are observed in $C_3$ species that are sister to $C_4$ clades of the eudicot genera *Heliotropium*, *Euphorbia*, *Cleome*, *Mollugo*, and some grasses (Marshall et al., 2007; Christin et al., 2011; Muhaidat et al., 2011; Sage et al., 2011b; Christin et al., 2013). Why $C_3$ species may initially develop a larger BS is unclear, but it may be related to the greater vein density of leaves in hot environments with high potential evapotranspiration (Sage, 2004; Osborne and Sack, 2012). High vein density increases hydraulic flux in such environments, thereby maintaining favorable leaf water status (Roth-Nebelsick et al., 2001; Scoffoni et al., 2011; Sage et al., 2012). Increasing vein density comes at the expense of M tissue, however, which could have a photosynthetic cost. Enlarged BS cells and organelle number are often associated with high vein density in arid-zone plants such as *Flaveria* spp., leading to the hypothesis that greater size and photosynthetic engagement of BS cells compensates for a reduction of M cells (Sage et al., 2012). With more photosynthetic activity, BS cells would also photorespire more, enhancing their Gly production. In these BS cells, the movement of mitochondria and chloroplasts to the inner BS could trap photorespiratory $CO_2$ and thus create the weak Gly shuttle that could offset photorespiratory costs in hot, low-$CO_2$ environments.

In conclusion, the demonstration that the $C_3$ sister species of $C_2$ clades in the genera *Heliotropium*, *Steinchisma*, and now *Flaveria* express proto-Kranz traits is strong evidence that the proto-Kranz condition is the critical initial phase in the evolution of $C_2$, and by extension, $C_4$, photosynthesis. Once the proto-Kranz traits are in place, benefits arising from the recycling of photorespiratory $CO_2$ could facilitate subsequent selection for greater flux of Gly into the inner BS. With increased organelle volume in the inner BS, there may arise a large enough sink for Gly such that a chance reduction of GDC expression in the M tissue would not be deleterious but would instead improve carbon gain in photorespiratory conditions. Upon establishment of the $C_2$ pathway, $C_4$ photosynthesis could follow because the Kranz-like features of the $C_2$ pathway may facilitate the up-regulation of the $C_4$ metabolic cycle (Sage et al., 2012). In short, the initial events that establish the proto-Kranz system could set in motion a

feed-forward, facilitation cascade that leads to $C_4$ photosynthesis. The high number of $C_4$ origins could thus reflect the relative ease of establishing the proto-Kranz condition and initiating such cascades.

## MATERIALS AND METHODS

### Plant Material

We studied sunflower (*Helianthus annuus*; $C_3$), *Sartwellia flaveriae* ($C_3$), and five *Flaveria* species, *Flaveria cronquistii* ($C_3$), *Flaveria pringlei* ($C_3$), *Flaveria robusta* ($C_3$), *Flaveria sonorensis* ($C_2$), and *Flaveria angustifolia* ($C_2$). We also included GDC immunolocalizations from *Flaveria floridana* ($C_2$) to facilitate comparison with the method of Hylton et al. (1988). Plants were grown from seeds or cuttings obtained from sources described in Supplemental Table S4. All plants were grown in a greenhouse in 20-L pots of a sandy-loam soil and were watered daily to avoid water stress. Fertilizer was supplied weekly as a 50:50 mixture of Miracle Grow 24-10-10 All Purpose Plant Food and Miracle Grow Evergreen Food (30-10-20) at the recommended dosage (22 mL of fertilizer salt per 6 L; Scotts Miracle-Gro; www.scotts.ca). Plants were trimmed every 4 to 8 weeks to minimize canopy crowding and maintain a balance between roots and shoots. For imaging and immunolocalizations, plants were sampled from 10 AM to 12 PM between April and October, when daylength was over 11.5 h and light intensity in the unshaded greenhouse regularly exceeded 1,400 $\mu$mol photons $m^{-2}$ $s^{-1}$. The youngest cohort of fully expanded leaves was sampled in full sun for all procedures used in the study.

### Leaf Anatomy, Ultrastructure, and Immunolocalizations

The internal anatomy of leaves was assessed on sections sampled from the middle of recent, fully expanded leaves (one leaf per plant; three to four plants per species). Samples were prepared for light and transmission electron microscopy as described by Sage and Williams (1995). For fixation, a 2% (v/v) $OsO_4$ solution was used in $C_3$ species and some of the intermediates; a 1% (v/v) $OsO_4$ concentration had to be used in $C_4$ plants and some $C_3$-$C_4$ intermediates due to overly dark staining of BS cells by the 2% solution. To quantify BS and M ultrastructural parameters, transmission electron microscopy images from 10 BS and M cells from each sampled leaf were analyzed using ImageJ software (National Institutes of Health; Schneider et al., 2012).

The preparation of tissue samples for the immunolocalization of Rubisco and GDCp was performed as described by Marshall et al. (2007). Polyclonal antisera used were anti-tobacco (*Nicotiana tabacum*) Rubisco (provided by N.G. Dengler, University of Toronto) and anti-pea (*Pisum sativum*) GDC (P-subunit from S. Rawsthorne's laboratory; Hylton et al., 1988). Controls for each enzyme immunolocalization method were conducted by omitting the antisera from the procedure; these showed no background stain in any tissue (Supplemental Figs. S2 and S4).

### Leaf Gas-Exchange Analysis

Gas-exchange measurements were conducted using a LI-6400 photosynthesis system (Li-Cor). The $C^*$ and $R_d$ were estimated by measuring the response of $A$ to $C_i$ at multiple light intensities (Laisk, 1977; Brooks and Farquhar, 1985). Light intensities used were saturating (1,400–1,000 $\mu$mol photons $m^{-2}$ $s^{-1}$), 400, 300, 200, 150, and 100 $\mu$mol $m^{-2}$ $s^{-1}$. The $C_i$ at which the initial slopes of the $A/C_i$ responses converged was taken as an estimate of $C^*$. The net $CO_2$ exchange rate corresponding to the convergence point was the estimate of $R_d$. All measurements were performed at 36°C to ensure high rates of Rubisco oxygenase activity. The $\Gamma$ (where $A$ is 0 $\mu$mol $m^{-2}$ $s^{-1}$) as a function of light intensity was determined for each species from the $A/C_i$ responses (Brooks and Farquhar, 1985).

Due to their relevance, we also include unpublished $\Gamma$ values at two light intensities from related $C_3$ and $C_2$ *Panicum* species (now *Steinchisma* and *Panicum* species; Aliscioni et al., 2003) determined during an earlier study of $C_2$ plants (Supplemental Table S3; Hylton et al., 1988).

### Data Analysis

Results were analyzed with Sigmaplot version 11.0 (Systat Software) using one-way ANOVA followed by the Student-Newman-Keuls multiple comparison test. For ultrastructural analysis, leaf samples were collected from three to four plants. For each parameter, the data from the 10 sampled images per plant were averaged to give one value for a plant. These individual plant values were the unit of replication for statistical analysis. For leaf gas exchange, four to 15 measurements were conducted on four to seven plants per species.

### Supplemental Data

The following materials are available in the online version of this article.

**Supplemental Figure S1.** Leaf cross sections of species in Flaveriinae.

**Supplemental Figure S2.** In situ immunolocalizations of Rubisco in leaves of *Flaveria* spp.

**Supplemental Figure S3.** In situ immunolocalizations of the P-subunit of the glycine decarboxylase complex in BS cells of leaves from *Flaveria* spp.

**Supplemental Figure S4.** In situ immunolocalization of the P-subunit of the glycine decarboxylate complex in M cells of leaves from *Flaveria* spp.

**Supplemental Table S1.** Number, size, and distribution of M cell organelles.

**Supplemental Table S2.** Individual species means for high-light $C_i$ at $R_d$ and $C^*$.

**Supplemental Table S3.** $CO_2$ compensation points of *Panicum* spp. and *Steinchisma* spp.

**Supplemental Table S4.** Collection information for species used in this study.

## ACKNOWLEDGMENTS

We thank Harold Brown, Gerry Edwards, Athena McKown, Mike Powell, and Erika Sudderth for providing seeds of the species used in this study.

Received May 8, 2013; accepted September 13, 2013; published September 24, 2013.

## LITERATURE CITED

**Aliscioni SS, Giussani LM, Zuloaga FO, Kellogg EA** (2003) A molecular phylogeny of *Panicum* (Poaceae: Paniceae): tests of monophyly and phylogenetic placement within the Panicoideae. Am J Bot **90:** 796–821

**Bauwe H, Keerbert O, Bassűner R, Parnik T, Bassűner B** (1987) Reassimilation of carbon dioxide by *Flaveria* (Asteraceae) species representing different types of photosynthesis. Planta **172:** 214–218

**Brooks A, Farquhar GD** (1985) Effect of temperature on the $CO_2/O_2$ specificity of ribulose-1,5-bisphosphate carboxylase oxygenase and the rate of respiration in the light: estimates from gas-exchange measurements on spinach. Planta **165:** 397–406

**Brown RH, Bouton JH, Rigsby L, Rigler M** (1983) Photosynthesis of grass species differing in carbon dioxide fixation pathways. VIII. Ultrastructural characteristics of *Panicum* species in the *laxa* group. Plant Physiol **71:** 425–431

**Brown RH, Hattersley PW** (1989) Leaf anatomy of $C_3$-$C_4$ species as related to evolution of $C_4$ photosynthesis. Plant Physiol **91:** 1543–1550

**Busch FA, Sage TL, Cousins AB, Sage RF** (2013) $C_3$ plants enhance rates of photosynthesis by reassimilating photorespired and respired $CO_2$. Plant Cell Environ **36:** 200–212

**Christin PA, Osborne CP, Chatelet DS, Columbus JT, Besnard G, Hodkinson TR, Garrison LM, Vorontsova MS, Edwards EJ** (2013) Anatomical enablers and the evolution of C4 photosynthesis in grasses. Proc Natl Acad Sci USA **110:** 1381–1386

**Christin PA, Sage TL, Edwards EJ, Ogburn RM, Khoshravesh R, Sage RF** (2011) Complex evolutionary transitions and the significance of $C_3$-$C_4$ intermediate forms of photosynthesis in Molluginaceae. Evolution **65:** 643–660

**Christin PA, Wallace MJ, Clayton H, Edwards EJ, Furbank RT, Hattersley PW, Sage RF, Macfarlane TD, Ludwig M** (2012) Multiple photosynthetic transitions, polyploidy, and lateral gene transfer in the grass subtribe Neurachninae. J Exp Bot **63:** 6297–6308

**Dai ZY, Ku MSB, Edwards GE** (1996) Oxygen sensitivity of photosynthesis and photorespiration in different photosynthetic types in the genus *Flaveria*. Planta **198:** 563–571

**Gerhart LM, Ward JK** (2010) Plant responses to low [$CO_2$] of the past. New Phytol **188:** 674–695

**Griffiths H, Weller G, Toy LF, Dennis RJ** (2013) You're so vein: bundle sheath physiology, phylogeny and evolution in $C_3$ and $C_4$ plants. Plant Cell Environ **36:** 249–261

**Hattersley PW, Wong SC, Perry S, Roksandic Z** (1986) Comparative ultrastructure and gas-exchange characteristics of the $C_3$-$C_4$ intermediate Neurachne minor S. T. Blake (Poaceae). Plant Cell Environ **9:** 217–233

**Holaday AS, Chollet R** (1984) Photosynthetic/photorespiratory characteristics of $C_3$-$C_4$ intermediate species. Photosynth Res **5:** 307–323

**Holaday AS, Lee KW, Chollet R** (1984) $C_3$-$C_4$ intermediate species in the genus Flaveria: leaf anatomy, ultrastructure and the effect of $O_2$ and $CO_2$ compensation concentration. Planta **160:** 25–32

**Hylton CM, Rawsthorne S, Smith AM, Jones DA, Woolhouse HW** (1988) Glycine decarboxylase is confined to the bundle sheath cells of leaves of $C_3$-$C_4$ intermediate species. Planta **175:** 452–459

**Kapralov MV, Kubien DS, Andersson I, Filatov DA** (2011) Changes in Rubisco kinetics during the evolution of $C_4$ photosynthesis in Flaveria (Asteraceae) are associated with positive selection on genes encoding the enzyme. Mol Biol Evol **28:** 1491–1503

**Ku MSB, Wu J, Dai Z, Scott RA, Chu C, Edwards GE** (1991) Photosynthetic and photorespiratory characteristics of *Flaveria* species. Plant Physiol **96:** 518–528

**Kubien DS, Whitney SM, Moore PV, Jesson LK** (2008) The biochemistry of Rubisco in *Flaveria*. J Exp Bot **59:** 1767–1777

**Laisk AK** (1977) Kinetics of Photosynthesis and Photorespiration in $C_3$ Plants. Nauka, Moscow

**Marshall DM, Muhaidat R, Brown NJ, Liu Z, Stanley S, Griffiths H, Sage RF, Hibberd JM** (2007) *Cleome*, a genus closely related to Arabidopsis, contains species spanning a developmental progression from $C_3$ to $C_4$ photosynthesis. Plant J **51:** 886–896

**McKown AD, Dengler NG** (2007) Key innovations in the evolution of Kranz anatomy and $C_4$ vein pattern in Flaveria (Asteraceae). Am J Bot **94:** 382–399

**McKown AD, Moncalvo JM, Dengler NG** (2005) Phylogeny of *Flaveria* (Asteraceae) and inference of $C_4$ photosynthesis evolution. Am J Bot **92:** 1911–1928

**Metcalfe CR, Chalk L** (1979) Anatomy of the Dicotyledons. Vol 1. Systematic Anatomy of the Leaf and Stem. Oxford Science Publishers, Oxford

**Monson RK, Edwards GE, Ku MSB** (1984) $C_3$-$C_4$ intermediate photosynthesis in plants. Bioscience **34:** 563–571

**Monson RK, Jaeger CH** (1991) Photosynthetic characteristics of $C_3$-$C_4$ intermediate *Flaveria floridana* (Asteraceae) in natural habitats: evidence of advantages to $C_3$-$C_4$ photosynthesis at high leaf temperatures. Am J Bot **78:** 795–800

**Monson RK, Rawsthorne S** (2000) Carbon dioxide assimilation in $C_3$-$C_4$ intermediate plants. *In* R Leegood, T Sharkey, S von Caemmerer, eds, Photosynthesis: Physiology and Metabolism. Advances in Photosynthesis. Kluwer Academic Press, Dordrecht, The Netherlands, pp 533–550

**Morgan JA, Brown RH** (1979) Photosynthesis in grass species differing in carbon dioxide fixation pathways. II. A search for species with intermediate gas exchange and anatomical characteristics. Plant Physiol **64:** 257–262

**Morgan JA, Brown RH** (1980) Photosynthesis in grass species differing in carbon dioxide fixation pathways. III. Oxygen response and enzyme activities of the *Laxa* groups of *Panicum*. Plant Physiol **65:** 156–159

**Muhaidat R, Sage TL, Frohlich MW, Dengler NG, Sage RF** (2011) Characterization of $C_3$-$C_4$ intermediate species in the genus Heliotropium L. (Boraginaceae): anatomy, ultrastructure and enzyme activity. Plant Cell Environ **34:** 1723–1736

**Osborne CP, Sack L** (2012) Evolution of C4 plants: a new hypothesis for an interaction of $CO_2$ and water relations mediated by plant hydraulics. Philos Trans R Soc Lond B Biol Sci **367:** 583–600

**Powell AM** (1978) Systematics of *Flaveria* (Flaveriinae, Asteraceae). Ann Mo Bot Gard **65:** 590–636

**Rawsthorne S** (1992) $C_3$-$C_4$ intermediate photosynthesis: linking physiology to gene expression. Plant J **2:** 267–274

**Rawsthorne S, Hylton CM, Smith AM, Woolhouse HW** (1988a) Photorespiratory metabolism and immunogold localization of photorespiratory enzymes in leaves of $C_3$ and $C_3$-$C_4$ intermediate species of *Moricandia*. Planta **173:** 298–308

**Rawsthorne S, Hylton CM, Smith AM, Woolhouse HW** (1988b) Distribution of photorespiratory enzymes between bundle-sheath and mesophyll cells in leaves of the $C_3$-$C_4$ intermediate species *Moricandia arvensis* (L.) DC. Planta **176:** 527–532

**Roth-Nebelsick A, Uhl D, Mosbrugger V, Kerp H** (2001) Evolution and function of leaf venation architecture: a review. Ann Bot (Lond) **87:** 553–566

**Sage RF** (2004) The evolution of $C_4$ photosynthesis. New Phytol **161:** 341–370

**Sage RF, Christin PA, Edwards EA** (2011a) The $C_4$ plant lineages of planet Earth. J Exp Bot **62:** 3155–3169

**Sage RF, Sage TL, Kocacinar F** (2012) Photorespiration and the evolution of $C_4$ photosynthesis. Annu Rev Plant Biol **63:** 19–47

**Sage TL, Sage RF, Vogan PJ, Rahman B, Johnson DC, Oakley JC, Heckel MA** (2011b) The occurrence of $C_2$ photosynthesis in *Euphorbia* subgenus *Chamaesyce* (Euphorbiaceae). J Exp Bot **62:** 3183–3195

**Sage TL, Williams EG** (1995) Structure, ultrastructure, and histochemistry of the pollen-tube pathway in the milkweed Asclepias exaltata L. Sex Plant Rep **8:** 257-265

**Schneider CA, Rasband WS, Eliceiri KW** (2012) NIH Image to ImageJ: 25 years of image analysis. Nat Methods **9:** 671–675

**Schulze S, Mallmann J, Burscheidt J, Koczor M, Streubel M, Bauwe H, Gowik U, Westhoff P** (2013) Evolution of $C_4$ photosynthesis in the genus *Flaveria*: establishment of a photorespiratory $CO_2$ pump. Plant Cell **25:** 2522–2535

**Schuster WS, Monson RK** (1990) An examination of the advantages of $C_3$-$C_4$ intermediate photosynthesis in warm environments. Plant Cell Environ **13:** 903–912

**Scoffoni C, Rawls M, McKown A, Cochard H, Sack L** (2011) Decline of leaf hydraulic conductance with dehydration: relationship to leaf size and venation architecture. Plant Physiol **156:** 832–843

**Sudderth EA, Espinosa-Garcia FJ, Holbrook NM** (2009) Geographic distribution and physiological characteristics of co-existing Flaveria species in south-central Mexico. Flora **204:** 89–98

**Tholen D, Ethier G, Genty B, Pepin S, Zhu X-G** (2012) Variable mesophyll conductance revisited: theoretical background and experimental implications. Plant Cell Environ **35:** 2087–2103

**Ueno O** (2011) Structural and biochemical characterization of the $C_3$-$C_4$ intermediate Brassica gravinae and relatives, with particular reference to cellular distribution of Rubisco. J Exp Bot **62:** 5347–5355

**Vogan PJ, Frohlich MW, Sage RF** (2007) The functional significance of C3-C4 intermediate traits in Heliotropium L. (Boraginaceae): gas exchange perspectives. Plant Cell Environ **30:** 1337–1345

**von Caemmerer S** (1989) A model of photosynthetic $CO_2$ assimilation and carbon-isotope discrimination in leaves of certain $C_3$-$C_4$ intermediates. Planta **178:** 463–474

**von Caemmerer S** (2000) Biochemical Models of Leaf Photosynthesis. Commonwealth Scientific and Industrial Research Organization, Collingwood, Australia

**Voznesenskaya EV, Koteyeva NK, Akhani H, Roalson EH, Edwards GE** (2013) Structural and physiological analyses in Salsoleae (Chenopodiaceae) indicate multiple transitions among C3, intermediate, and C4 photosynthesis. J Exp Bot **64:** 3583–3604

**Voznesenskaya EV, Koteyeva NK, Chuong SDX, Ivanova AN, Barroca J, Craven LA, Edwards GE** (2007) Physiological, anatomical and biochemical characterisation of photosynthetic types in genus *Cleome* (Cleomaceae). Funct Plant Biol **34:** 247–267

**Voznesenskaya EV, Koteyeva NK, Edwards GE, Ocampo G** (2010) Revealing diversity in structural and biochemical forms of $C_4$ photosynthesis and a $C_3$-$C_4$ intermediate in genus *Portulaca* L. (Portulacaceae). J Exp Bot **61:** 3647–3662